**Supplementary Information**

# Direct delivery of MRI contrast through skull vessel/marrow pathways into the brain guided by microCT

Li Liu[1,*], Martin J. MacKinnon[1], Tatjana Atanasijevic[1], Stephen Dodd[1], Nadia Bouraoud[1], Danielle Donahue[2], Harikrishna Rallapalli[1], Alan P. Koretsky[1,*]

[1]Section on Plasticity and Imaging of the Nervous System, Laboratory of Functional and Molecular Imaging, National Institute of Neurological Disorders and Stroke, National Institutes of Health, Bethesda, MD 20892, USA.

[2]Mouse Imaging Facility, National Institute of Neurological Disorders and Stroke, National Institutes of Health, Bethesda, MD 20892, USA.

*Corresponding to: li.liu3@nih.gov; koretskya@ninds.nih.gov.

| Figure | Experiment | Animal Number |
|---|---|---|
| 1 | Quantification of volume ratio of channel (total of skull surface to brain and brain to skull) to bone and marrow to bone | 6 |
| 2 | H and E staining of rat skull bone | 6 |
| 4 | $Mn^{2+}$ can be delivered efficiently through “short paths” | |
| | $Mn^{2+}$ delivery | 5 |
| | Saline control | 4 |
| 5 | $Mn^{2+}$ can be delivered efficiently through intact skull above the cerebellum | |
| | $Mn^{2+}$ delivery | 6 |
| | Saline control | 4 |
| 6 | Minimum thinning skull can increase the delivery efficiency | |
| | $Mn^{2+}$ delivery | 6 |
| | Saline control | 6 |
| Supplementary Video 1 | The reconstructed 3D microCT image to show the intricate geometry of vessel/marrow paths. | 1 |
| S1 | MicroCT of bottom skull of a rat, especially under the olfactory bulb and forebrain, showed a large volume of marrow | 3 |
| S2 | H and E staining of rat skull bone and femur bone marrow | 1 |
| **Total** | | **48** |

**Table S1.** Animal number used in each experiment.

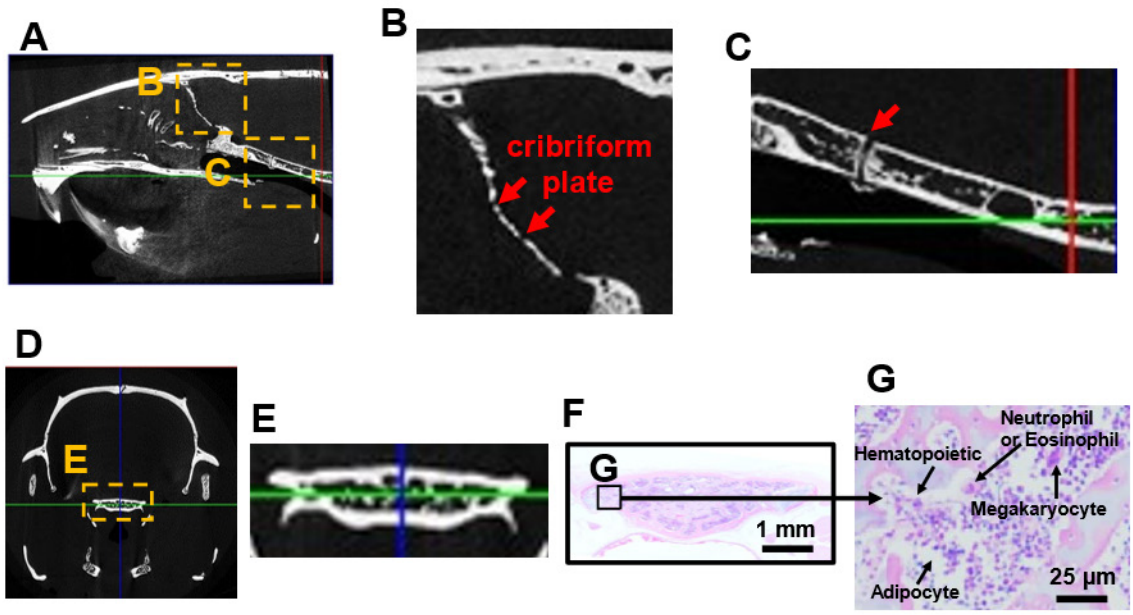


**Figure S1.** Bottom skull of a rat, especially under the olfactory bulb and forebrain, showed a large volume of marrow. (**A-C**) microCT images of sagittal view of bottom skull. (**D, E**) microCT images of coronal view of bottom skull. (**F, G**) H & E staining of the marrow in the bottom skull.

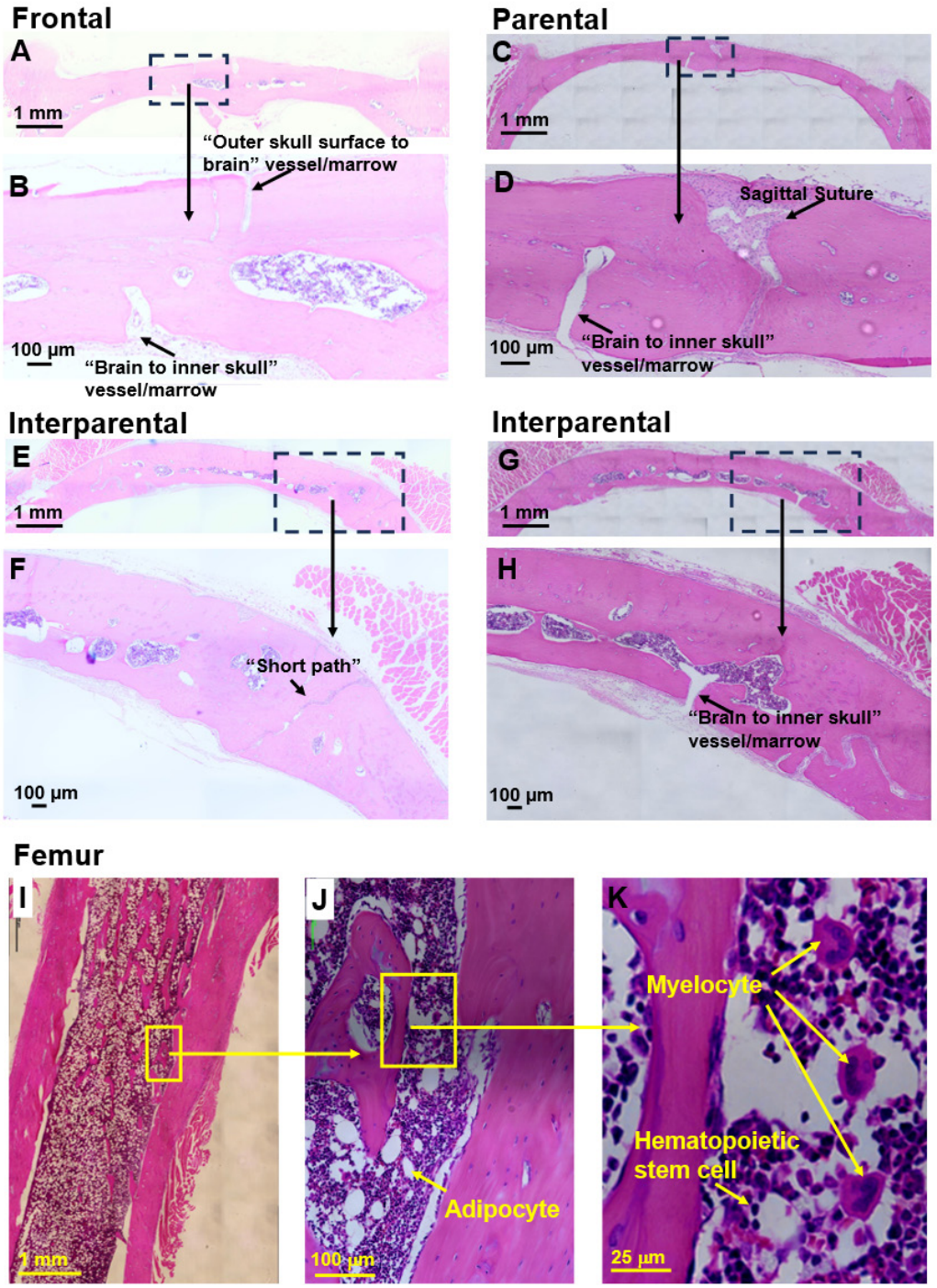


**Figure S2.** H and E staining of rat skull bone and femur bone marrow. (**A,B**) Frontal bone. (**C,D**) Parietal bone. (**E-H**) Interparietal bone. (**I-K**) Femur bone.

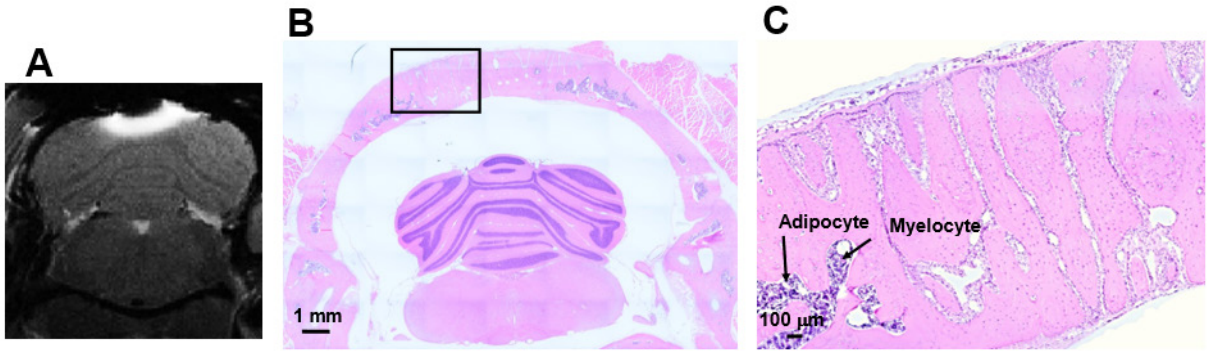


**Figure S3.** Efficient delivery of $Mn^{2+}$ through intact skull above the cerebellum by using the skull/marrow pathways. (**A**) Representative views of $T_1$-weighted MRI of cerebellum 2-hr post $Mn^{2+}$ application. (**B, C**) H and E staining of the skull-brain tissue at the cerebellum to show the skull vessel/marrow pathways.

**Data Availability Statement**

**Figure-Data-List through Figshare**
**Link:** https://figshare.com/s/0c348af11fb86ab9e9b1

**Figure 1.Zip High-resolution microCT of a rat top skull showing an intricate geometry of vessel/marrow paths connecting the outer skull surface and meninges.**
**Link:** https://figshare.com/s/5fb97feeef60a24f36a0
**Figure-1-(A-K)** Coronal views of high-resolution microCT of a rat top skull and the reconstructed 3D image to show the intricate geometry of vessel/marrow paths.
**Figure-1-(L-O)** Quantification of volume ratio of channel (total of skull surface to brain and brain to skull) to bone and marrow to bone.

**Figure 3.Zip Human skull also shows vessel/marrow pathways connecting outer skull surface and meninges, as reviewed by high-resolution CT.**
**Link:** https://figshare.com/s/c8a42bf566d25bd3e719
**Figure-3-(A-H)** Coronal views of high-resolution CT of a human skull shows vessel/marrow pathways connecting outer skull surface and meninges.
**Figure-3-I** Quantification of the diameters of skull channels (not including suture line areas) of human skull and rat skull.

**Figure 4.Zip $Mn^{2+}$ can be delivered efficiently through "short paths".**
**Link:** https://figshare.com/s/ed5759286245f9499ace
**Figure-4-B** Representative $T_1$-weighted MRI to show that $Mn^{2+}$ can be delivered efficiently through "short paths".
**Figure-4-D** Data for the quantification of the average median and $90^{th}$ percentile of the contrast-to-noise ratio (CNR) of the enhanced area.
**Figure-4-E** Data for the quantification of T1 enhanced volume.

**Figure 5.Zip $Mn^{2+}$ can be delivered efficiently through intact skull above the cerebellum.**
**Link:** https://figshare.com/s/8e8fa297fd8e93d59a9f
**Figure-5-B** Representative $T_1$-weighted MRI to show that $Mn^{2+}$ can be delivered efficiently through intact skull above the cerebellum.
**Figure-5-D** Data for the quantification of the average median and $90^{th}$ percentile of the contrast-to-noise ratio (CNR) of the enhanced area.
**Figure-5-E** Data for the quantification of T1 enhanced volume.

**Figure 6.Zip Minimum thinning skull on the top of "brain to skull" vessel/marrow pathways can increase the delivery efficiency.**
**Link:** https://figshare.com/s/b7076ed02275184a0f4c
**Figure-6-B** Representative $T_1$-weighted MRI to show that minimum thinning skull on the top of "brain to skull" vessel/marrow pathways can increase the delivery efficiency.
**Figure-6-E** Data for the quantification of the average median and $90^{th}$ percentile of the contrast-to-noise ratio (CNR) of the enhanced area.

**Figure-6-F** Data for the quantification of T1 enhanced volume.

**Supplementary Video 1.** The reconstructed 3D microCT image to show the intricate geometry of vessel/marrow paths.
**Link:** https://figshare.com/s/e506d8567974069184a9